Canadian Journal of
Forest Research

OPEN ACCESS | Research Article

Can forest management inventory support national forest inventory to improve the municipal-level estimation of timber volume?

Janne Räty[a], **Mikko Kukkonen**[b], **Annika Kangas**[a], **Jacob Strunk**[c], **Raisa Mäkipää**[d], **and Petteri Packalen**[e]

[a]Natural Resources Institute Finland, Bioeconomy and Environment, Forest Inventory and Planning, Yliopistokatu 6, 80100 Joensuu, Finland; [b]Natural Resources Institute Finland, Bioeconomy and Environment, Forest Inventory and Planning, Paavo Havaksen tie 3, 90570 Oulu, Finland; [c]PotlatchDeltic, Forest Inventory and Planning, Spokane, WA 99201, USA; [d]Natural Resources Institute Finland, Bioeconomy and Environment, Carbon Cycle Management, Latokartanonkaari 9, 00790 Helsinki, Finland; [e]Natural Resources Institute Finland, Bioeconomy and Environment, Forest Inventory and Planning, Latokartanonkaari 9, 00790 Helsinki, Finland

Corresponding author: **Janne Räty** (email: janne.raty@luke.fi)

Abstract

National forest inventories (NFIs) provide unbiased statistics for forest resource monitoring. Since NFIs primarily target large areas, they are less effective for small areas, such as municipalities, due to low sampling intensity and precision. In Finland, forest management inventories (FMIs) provide stand-level information but are biased for domain-level estimations. We evaluated a model-assisted estimator that used NFI plots integrated with FMI plots for municipal-level estimations. We used linear and tree-boosting models in 619 synthetic municipalities. The assisting models had a fixed set of nine predictor variables extracted from aerial image-based point clouds and Sentinel-2 images. Our findings indicated that the assisting models that used FMI field plots did not show improved efficiency over models fitted with the NFI plots in the 20 km buffer zone that surrounded the municipality of interest. The model-assisted estimators explained 66%–69% of the variation of the NFI field data-based mean estimates. A modest improvement was feasible by fitting a model that used both NFI and FMI plots, although the marginal precision improvements achieved and the additional effort required to harmonize the FMI plots with the NFI plots was not justified.

Key words: small area estimation, photogrammetric point clouds, difference estimator

Introduction

National forest inventories (NFIs) play a critical role in the monitoring of forest resources and serve society by providing information that ranges from timber availability to forest biodiversity and carbon sink potential. Typically, NFIs rely on a probability sample of field plots that allow for design-unbiased estimation of forest attributes at national and regional scales (e.g., a municipality in Finland). Model-based estimators that leverage the statistical relationships between remotely sensed attributes and forest attributes have been suggested as an approach to improve estimation precision for small populations, such as municipalities (Breidenbach and Astrup 2012; Mäkisara et al. 2022). The current needs of municipalities that aim to reach carbon neutrality (e.g., Karhinen et al. 2021) or large forest owners, who report their societal responsibility and contribution to forest carbon sinks, require methods to assess forest attributes in small areas. In many practical applications, a design-based estimator is preferred over a model-based estimator because the latter approach can be highly biased. However, design-based estimators may exhibit poor precision in small geographical domains due to a small number of field plots in the region of interest. The issue of poor precision can be mitigated to some degree through integration of auxiliary information, such as remotely sensed data, into an estimation framework. Model-assisted techniques incorporate auxiliary information into the estimation framework through a fitted model that can increase estimation precision. For example, forest attribute maps produced using satellite images and NFI data have been integrated into estimation frameworks with a regression estimator (Opsomer et al. 2007; Saarela et al. 2015; Puliti et al. 2021).

The model-assisted framework can adopt complex models that take advantage of various sources of auxiliary information as long as the auxiliary variables are sufficiently correlated with the target attributes in the domain of interest (Myllymäki et al. 2017). A limitation of model-assisted estimation is that there may be too few plots or no plots at all in a spatial subdomain (or subregion) of interest. Estimation within spatial subdomains is commonly referred to as small area estimation. For cases with few or no plots in the spatial subdomains, the assisting model can still be leveraged to generate a prediction for the small area, which results in model-based inferences in the spatial subdomain of interest. This is not an optimal solution, as the estimator will not be unbiased in the spatial subdomain, and the properties of the estimator may be difficult to assess (Kangas et al. 2025). Regardless, it is worth noting that model-based estimation is often the only option in the smallest spatial subdomains, such as forest stands or watersheds, but its use for long-term decision-making should be approached with caution. This study mainly focuses on the model-assisted estimators and their assisting models in subdomains that have sufficient field plots for a design-based inference. To evaluate the effectiveness of assisting models as model-based estimators, we investigated how often estimates produced using assisting models (i.e., pixel-counting estimates) fall within the confidence intervals (CIs) of a model-assisted estimate.

A challenge associated with the application of model-assisted estimators in NFIs is related to the estimator variance. The sampling network of the NFI typically covers the subdomain of interest (e.g., a municipality), and the use of field plots in the municipality to both fit an assisting model and estimate sampling variation is the most affordable option. However, the use of the same sample of field plots for both model fitting and variance estimation results in underestimates of sampling variation (Massey et al. 2014; Kangas et al. 2016). This is mostly attributable to the overfitting of assisting models. While the risk of underestimation could be mitigated to some extent with careful model formulation, fitting the assisting model independently of the sample used for variance estimation is the preferred approach (McRoberts et al. 2022).

In Finland, forest management inventories (FMIs) are part of a continuous national inventory program organized by the Finnish Forest Centre specifically for forest management applications. The Finnish FMI is a separate program independent of the NFI. The objective of the NFI is to provide unbiased monitoring of forest resources over large areas, while the FMI system is designed to provide stand-level information for the purposes of operational forestry (Maltamo and Packalen 2014). The FMI sample plot placement is nonrandom within a municipality and is instead focused on representation of stand-level conditions in forests with active timber management. The FMI is temporally synchronized with the national collection of aerial imagery and airborne laser scanning (ALS) data. To support this process, Finland is divided into inventory blocks that are used to separate and organize the inventory work and data acquisition. Field measurements, aerial imagery, and ALS data are all acquired for an inventory block in approximately the same year. From the standpoint of small area estimation in Finnish NFIs, FMI field plots offer a promising data source to fit assisting models because they are collected independently of the NFI and could be used to localize modeling efforts. The FMI assisting models could then be used with the independent NFI plots for exactly design-unbiased estimation (e.g., Särndal et al. 1992, p. 222, eq. 6.3.4). When the same set of sample plots is used for both model fitting and estimation, the model-assisted estimator is only asymptotically design-unbiased (Särndal et al. 1992; McRoberts et al. 2022, p. 225). A downside of this approach is that the FMI-based assisting model may perform poorly for forests that are not under active forest management as no plots are collected from conserved or poorly growing forests.

Medium-resolution satellite images provided by Copernicus Sentinel-2 are often used for the model-assisted inference as they are free to access, relatively fine grain size (10–20 m), and have a high temporal frequency over large regions (Haakana et al. 2020; Puliti et al. 2020). Satellite images have, however, limited capacity to explain the variability in forest attributes relative to remote sensing sources, such as ALS or photogrammetry, which can provide three-dimensional forest structure (Hawryło and Wężyk 2018; Irulappa-Pillai-Vijayakumar et al. 2019). Derivatives of three-dimensional structure, especially tree height and cover information, are more closely associated with aggregate tree biomass-related attributes than spectral reflectance recorded by satellite cameras. In practical forest-inventory applications that use three-dimensional remote sensing, the data are typically collected with sensors mounted on a fixed-wing airborne platform. Photogrammetric point clouds derived from airborne imagery are, in general, considerably less expensive than ALS acquisitions (Bohlin et al. 2012; Rahlf et al. 2017). In part due to its lower cost, national-level airborne imagery is collected every 3 years in Finland. The increased temporal resolution of the photogrammetric point clouds has made them an appealing dataset to support forest inventories.

While photogrammetric point clouds are considerably less expensive than ALS data, a number of studies have demonstrated that, compared to ALS data, they explain less of the variation observed in forest attributes (e.g., Bohlin et al. 2012; White et al. 2013; Pitt et al. 2014; Rahlf et al. 2017). While several studies have demonstrated improved efficiencies with photogrammetric point clouds in a design-based context, the performance of photogrammetric point clouds in a small-area estimation context is not well described in the literature. Pulkkinen et al. (2018) used photogrammetric point clouds post-stratification (i.e., model-assisted estimation) in the Swiss NFI, which improved the efficiency of forest area and volume estimates by 81% and 34%, respectively. Irulappa-Pillai-Vijayakumar et al. (2019) applied model-assisted estimations using a *k* nearest neighbor's model with photogrammetric point cloud metrics as predictor variables and achieved a precision improvement of 49% for volume in complex broadleaf-tree dominated forests. Schroeder et al. (2022) reported that post-strata estimates from photogrammetric point clouds were, on average, 31% more precise than estimates based on national tree canopy cover maps created from satellite imagery.

In this study, we used re-sampling simulations to investigate design-based properties of the estimators in the domains of small area estimation. Our re-sampling simulations mimic municipalities that are used to carry out municipal-level estimation of timber volume using auxiliary photogrammetric point clouds related to both NFI and FMI plots with assisting models. This investigation motivated us to evaluate the following research questions:

1. Can probabilistic and nonprobabilistic samples be integrated to more efficiently estimate forest attributes relative to the probability sample alone in a model-assisted framework?
2. How does localization of assisting models, and modeling techniques (linear regression vs. tree-boosting) affect the efficiency of model-assisted timber volume estimators?
3. Do the most important predictor variables in the localized models vary between municipalities?
4. How often do the volume estimates produced using only the assisting model, i.e., model-based estimates, fall within the 95% CIs of model-assisted estimates?

Materials and methods

Study area

The study area was a 1.56 million ha region located in central Finland (Fig. 1). This region falls completely inside a single NFI sampling region (Korhonen et al. 2024). The study area overlaps six different blocks from the spatially coincident FMI field plot and aerial imaging campaigns (National Land Survey of Finland 2025). Field plots and remote sensing acquisitions for the FMI blocks are on a continuous 6-year return cycle in which one-sixth of blocks are collected each year. However, FMI blocks do not match spatially or temporally with NFI sampling regions, which means that the total size of the FMI blocks that intersect the study area is larger than the study area.

Forests in the study area are dominated by coniferous tree species: Scots pine (*Pinus sylvestris* [L.]) and Norway spruce (*Picea abieas* [L.] Karst.). Broadleaved species, such as birch (*Betula* spp.), are common as mixtures. The forests within the study area are used for multiple functions of which timber production is typically the major interest. Forest management practices aimed at timber production, such as clearcutting and thinning, influence forest structure and landscape, and result in greater variability in structure than would be seen naturally. As a result, the forest landscape is a mosaic of different structural and developmental conditions.

Finnish NFI data

We used field measurements from the 13th Finnish NFI (Korhonen et al. 2024) that were collected from 2019 to 2023. The Finnish NFI uses a systematic cluster sampling design in which each cluster contains 8–11 concentric, circular field plots (Korhonen et al. 2024). Trees with a diameter at breast height (dbh) $\geq$ 9.5 cm are measured in field plots with a radius of 9 m, whereas trees with 4.5 cm $\leq$ dbh < 9.5 cm are recorded in field plots with a radius of 4 m. We did not consider trees with dbh values < 5 cm in this study to harmonize NFI-measured forest attributes with the FMI inventory protocol. The NFI trees were measured either as tally trees or sample trees (i.e., represent a sub-sample of the tally trees). From the point of view of this study, the most relevant tally tree measurements were dbh and species, whereas the sample tree measurements also comprised tree height. The heights of the tally trees were predicted using multivariate diameter-height models, as described in Korhonen et al. (2024). Both dbh and tree height were projected to the year 2021, the midpoint of the inventory cycle. Projections were performed with in-house projection models that were based on the species-specific (i.e., pine, spruce, deciduous) growth rates of dbh and estimated based on core samples associated with NFI sample trees. We computed stem volume for each tree using the species-specific volume models presented in Kangas et al. (2022). We employed the forest mask used in the multi-source NFI (Mäkisara et al. 2022). Our study area included 3651 NFI plots, of which 2642 were classified as forest according to this mask. We considered the forest mask values as true values, which means that we evaluated the performance of the estimators exactly in the forest populations for which the assisting models were used to produce predictions. Thus, the effect of errors associated with the forest mask on estimator performance is beyond the scope of this study. Statistics associated with NFI data both in the forests determined by the forest mask and field observations are shown in Table 1.

FMI data

The FMI field plots measured between 2019 and 2023 were obtained from the publicly available database provided by the Finnish Forest Center (Metsäkeskus 2024). The Finnish FMI uses circular field plots with a radius of either 9 or 12.62 m (depending upon the number of trees per hectare) for young, middle-aged, and mature forests. The larger plot size is most commonly selected in mature forests, which tend to have fewer trees per hectare. For seedling and sapling plots, a fixed radius 5.64 m plot was used. In addition to the circular plots, the Finnish FMI also uses so-called “tree map plots” of which all trees are positioned and measured in the field. The trees are also delineated using ALS data post-processing. Due to the tree-level presentation, tree map plots do not have fixed shape or size, and cover a larger area than the aforementioned circular field plots. Tree map plots were harmonized with the other plot data by intersecting a circular plot (5.64, 9, or 12.62 m radius depending on tree size and number of stems per hectare) with mapped tree locations, and only using trees that occurred within the circular plot. The Finnish Forest Center determines the placement of the FMI plots based on pre-information, such as existing forest attribute maps and inventory databases. The set of the FMI plots is not a probability sample. Field plots were accurately positioned with a global navigation satellite system (GNSS) device, followed by differential post-correction (Erenoglu 2017). The FMI field plots, which are focused on actively managed sites, served as training data for models used by the Finnish Forest Center to produce forest attribute maps for the purposes of operational forestry. In total, we used 3151 FMI field plots in this study (Table 1).

Remotely sensed data

Aerial images were sourced from the National Land Survey (NLS) of Finland. For the acquisition of national remote sensing data, Finland is divided into approximately 100 inventory blocks. Our study area consisted of six inventory blocks. Individual block size is variable across the country and was

Fig. 1. Location of the study area and field plots. The figure was created using QGIS version 3.44.7 (https://qgis.org/) and assembled from the Natural Earth data (naturalearthdata.com). NFI – national forest inventory; FMI – forest management inventory.

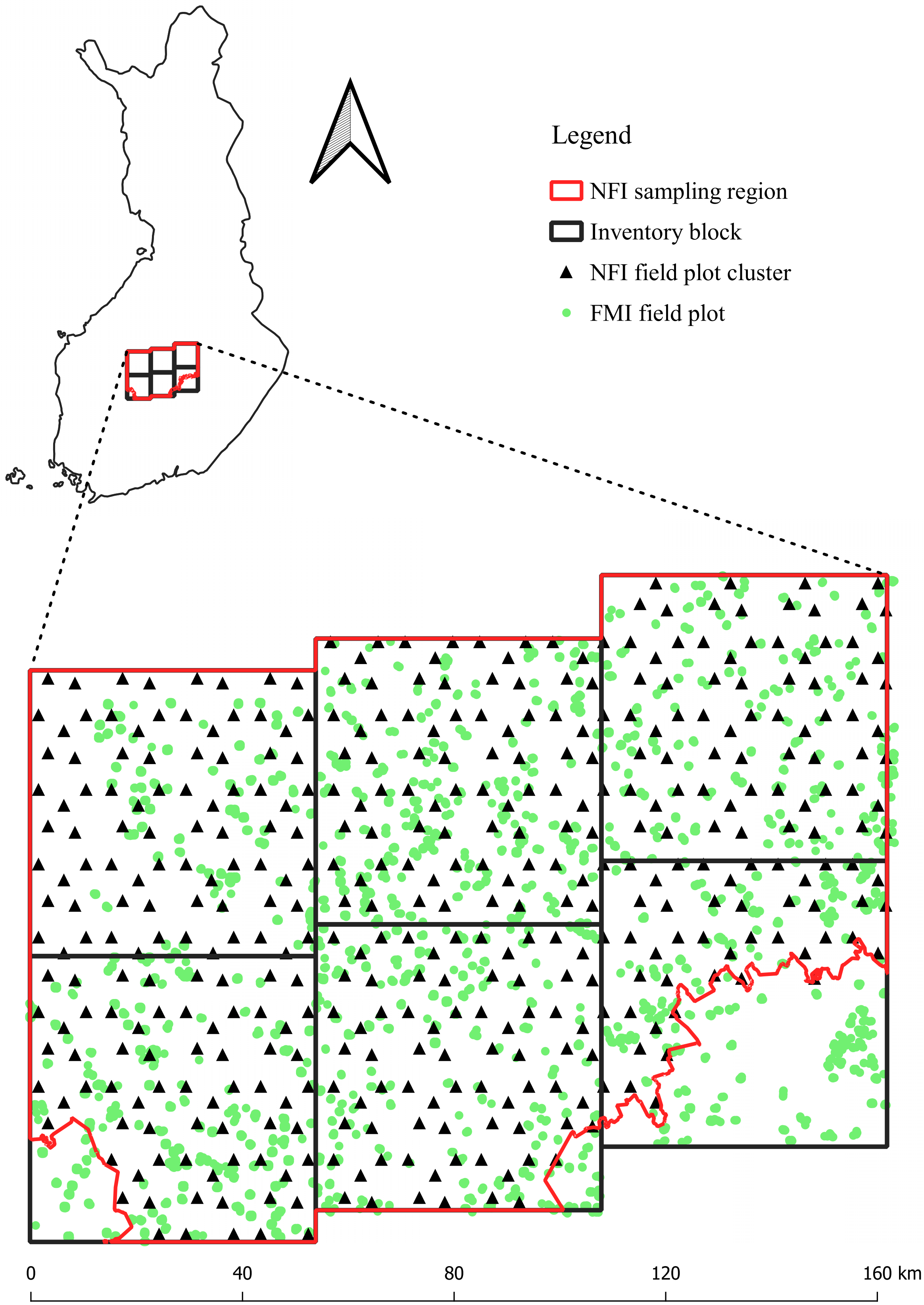

Table 1. Volume statistics associated with the national forest inventory (NFI) and forest management inventory (FMI) field plots.

Data	Mean volume (m^3/ha)	25th percentile of volume (m^3/ha)	Median of volume (m^3/ha)	75th percentile of volume (m^3/ha)	SD of volume (m^3/ha)	Maximum volume (m^3/ha)
NFI in forest (based on field observations)	147.94	64.21	127.62	204.80	116.31	987.68
NFI in forest (based on the forest mask)	140.24	51.68	120.92	198.40	117.42	987.68
FMI	135.78	56.65	116.84	191.93	113.65	703.83

Note: Trees with a diameter at breast height (dbh) greater or equal to 5 cm were considered. SD—standard deviation.

Table 2. Description of image data acquisitions in the study area.

Block	Date	Sensor	GSD (cm)	Altitude (m)
Tervo	24 June 2022	UltraCam Eagle Mark 3	30	7538
Jyväskylä	23 May 2020	UltraCam Eagle Mark 2	40	6939
Äänekoski	14 June 2020	UltraCam Eagle Mark 1	40	7731
Pieksämäki	21 May 2022	UltraCam Eagle Mark 2	40	6939
Saarijärvi	30 May 2021	UltraCam Eagle Mark 2	40	6939
Keuruu	18 June 2021	UltraCam Eagle Mark 3	30	7538

Note: GSD—ground sampling distance.

approximately 292 000 ha in our study area. Each year, images are captured from a subset of approximately 33% of the blocks both by NLS and private contractors. Camera configurations and the time window of data acquisitions within years can vary between blocks. The forward and side laps were 80% and 30%, respectively, for all blocks. The operational collections alternate between leaf-on and leaf-off conditions. We used only the most recent data for this study area, which were all leaf-on data. The ground sampling distances were either 30 or 40 cm. Images were acquired between 2020 and 2022. A detailed description is presented in Table 2.

The collection of FMI field plots was synchronized with the acquisition of the national ALS data over a 6-year period, while aerial images are collected over a shorter 3-year period. This means that the dates of the most recent FMI plot data may diverge by up to 3 years from the most recent image collection dates.

Agisoft Metashape (Agisoft 2024) was used to create point clouds for the study area using automated photogrammetric processing. The photogrammetric point cloud was created using the software's "High" quality and "Mild" filtering settings. The exterior and interior orientations of the images were optimized by NLS in a separate process (not in Agisoft Metashape), which included precise camera calibration and a bundle block adjustment that used a comprehensive set of ground control points.

Photogrammetric point clouds were clipped for both NFI and FMI field plots and used to compute height distribution metrics. These were paired with field-measured forest attributes for forest modeling. The height metrics derived included mean (hmean), median (hmed), height standard deviation (zsd), quantiles (z5, z10, …, z95), and proportions of points below fixed heights of 1.3, 2.5, 5.0, 10.0, 15.0, 20.0, and 25.0 m (p1.3, p2, …, etc.). Similar metrics were also computed wall-to-wall in the study area using a 16 m grid cell size.

We incorporated multispectral information into the modeling using a manually constructed mosaic of Sentinel-2 images, as described in Pitkänen et al. (2024). The Sentinel-2 Level-2A images acquired for the study area in June 2020 and July 2021 were downloaded from the Copernicus Open Access Hub (Copernicus Data 2023). Images were screened for heavy cloud cover with the provided masks, and then manually screened for clouds using visual inspections. The mosaic was resampled to a pixel size of 10 m using the nearest neighbor method. The Sentinel-2 bands of interest were B2 (blue), B3 (green), B4 (red), B5 (red edge), B6 (red edge), B7 (vegetation red edge), B8 (near-infrared), B8A (near-infrared), B11 (shortwave-infrared), and B12 (shortwave-infrared). The S2 metrics were computed as area-weighted means for the NFI and FMI field plots by the S2 bands (s2b2, s2b3, …, etc.). A similar set of Sentinel-2 metrics were also computed for all population elements in the study area using a 16 m grid cell size.

Generation of synthetic municipalities

We delineated the study area into synthetic municipalities using a region-growing procedure. We first tessellated the study area into a regular square grid with a cell size of 1440 m × 1440 m. The tessellation of the study area was repeated 60 times (four examples are shown in Fig. 2). Next, seed points for the individual municipalities were randomly placed within the study area. The locations of seed points were restricted to be a minimum of 25 km apart from each other. The grid cells that contained a seed point ("seed cell") were assigned a unique ID for that municipality. At each iteration of region-growing, the geographically closest grid cells of each seed were assigned to that municipality. To simulate a unique shape for each municipality (typical in Finland), the location of the seed point was randomly shifted during iterations. Region-growing was iterated until all the grid cells in

Fig. 2. Examples of synthetic municipalities in the study area generated using the region-growing procedure. The border lines of the southeastern municipalities follow the sampling region of the Finnish National Forest Inventory. The figure was created using QGIS version 3.44.7 (https://qgis.org/).

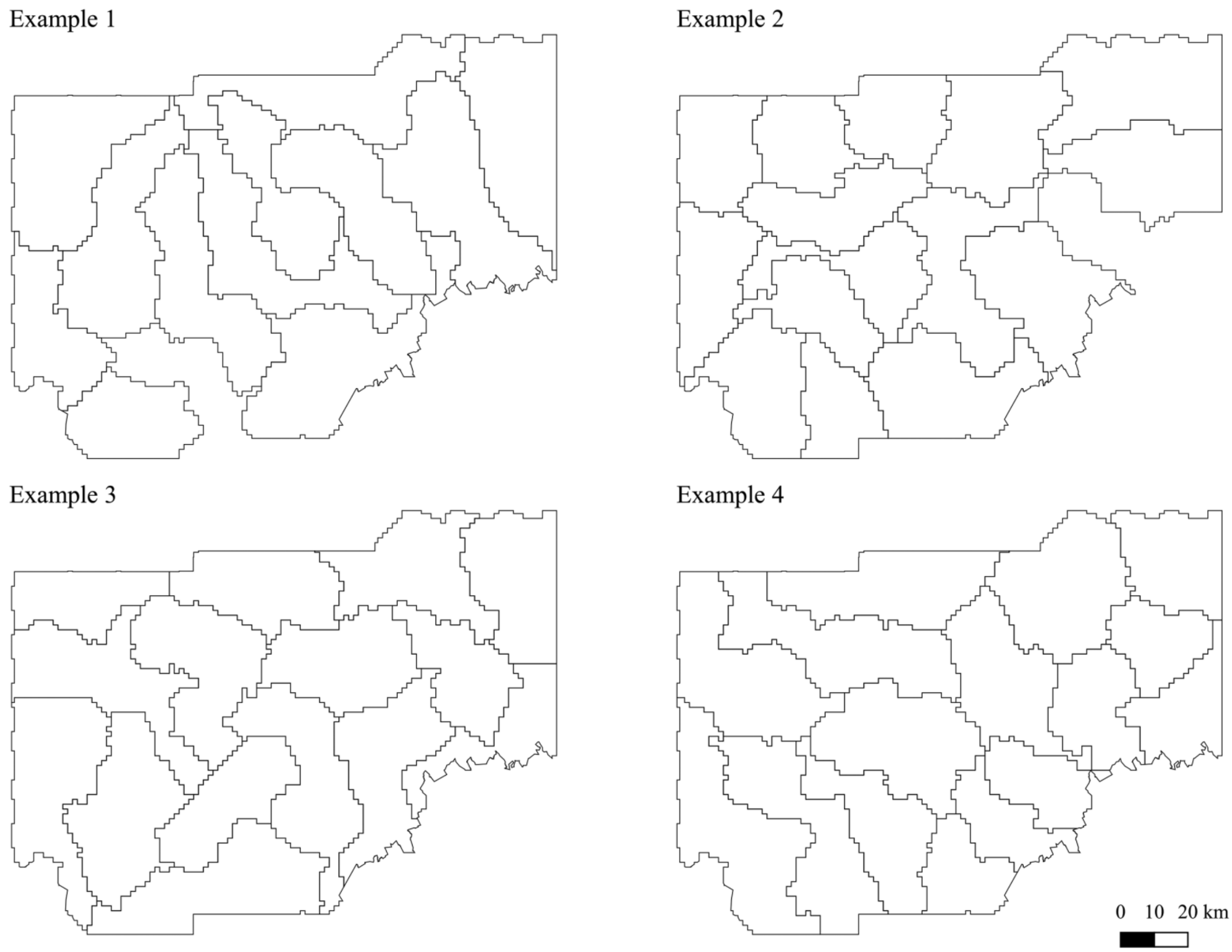

the study area were designated to a municipality. The region-growing procedure was constrained so that NFI plot clusters of 9–11 plots all fell within a single simulated municipality. We carried out the region-growing procedure 60 times, which produced 911 synthetic municipalities with a mean geographical area of 971 km^2.

Assisting models

Multiple linear regression models (LMs) served as reference assisting models in this study. We fitted LMs for timber volume using ordinary least squares regression. We square-root transformed the response variable to avoid negative predictions. The square-root transformed predictions were back-transformed. The bias caused by transformation was corrected by adding the squared standard error of the residuals to the predicted volumes (Mehtätalo and Lappi 2020, p. 317). In addition to the reference linear model, we also used a linear mixed-effects model (mixed-effects model) to account for the between-municipality variation in the study area. Mixed-effects model models with a random intercept were fitted using the *nlme* package (Pinheiro et al. 2025) in the R environment (R Core Team 2025).

In our simulations, a single fixed set of nine predictor variables was used in all fitted models to eliminate the effect of variable selection on model performances. The set of nine predictor variables was selected manually using a combination of expert opinion and backward selection. First, the global LM with all variable candidates was fitted, and then based on the initial model, we removed (with backward selection) insignificant predictor variables (5% significance level). The final set of predictor variables was selected with expert opinion from the significant predictors. The following set of predictor variables was used for all models fitted in this study: zsd, z95, p1.3, p5.0, p15.0, s2b10, s2b2, s2b3, and s2b8A.

For multiple regression, the model was formulated as follows:

$$\sqrt{y_i} = \beta_0 + \beta_1 x_{1i} + \cdots + \beta_9 x_{9i} + e_i \tag{1}$$

where variables x_{1i} … x_{9i} are the nine remote sensing explanatory variables. For the mixed effects model, we added an additional term, $l_i \sim N\left(0, {\sigma_l}^2\right)$, which represented the

Table 3. Description of the assisting models used in the model-assisted estimator.

Model type	Abbreviation	Field data	Description
Linear	$LM_{FMI,glo}$	FMI	Global models fitted to a plot in all municipalities
XGBoost	$XGB_{FMI,glo}$		
Linear	$LM_{FMI,loc}$	FMI	Local models fitted to plots in the municipality of interest
XGBoost	$XGB_{FMI,loc}$		
Linear	$LM_{NFI,loc}$	NFI	Local models fitted to plots in a 20 km buffer that surround the municipality
XGBoost	$XGB_{NFI,loc}$		
Linear mixed-effects	$LME_{FMI,me}$	FMI	Global mixed effects models with a random intercept for the municipality
GPboost	$GPB_{FMI,me}$		
Linear	$LM_{NFI,FMI,loc}$	FMI and NFI	Local models fitted to combined plot FMI and NFI datasets in a 20 km buffer that surround the municipality
XGBoost	$XGB_{NFI,FMI,loc}$		

Note: FMI—forest management inventory, NFI—national forest inventory, glo—global, loc—local, me—mixed effects. LM – linear regression model; XGBoost – Extreme Gradient Boosting; LME – linear mixed effect.

municipality-specific (group) random intercept.

$$\sqrt{y_i} = \beta_0 + \beta_1 x_{1i} + \cdots + \beta_9 x_{9i} + l_i + e_i \tag{2}$$

Tree-boosting machine-learning models were also evaluated, using the same set of nine predictor variables as in the LMs. We evaluated Extreme Gradient Boosting (XGBoost) and GPboost algorithms (Fabio et al. 2021; Chen et al. 2025): the former is a gradient-boosting algorithm that constructs an ensemble of decision trees sequentially, while the latter extends XGBoost by integrating random effects into the tree-boosting framework. This enables the boosting model to capture the variability associated with groups (here, municipalities), similar to our use of mixed effects in the case of linear regression.

The tree-boosting models were optimized by their hyperparameters using a grid search algorithm and leave-five-out cross validation. The parameters optimized for the XGBoost models were tree depth, loss reduction, and learn rate. The optimization of the XGBoost model was carried out using automatic grid space filling and model tuning in the *tune* R package (Kuhn 2025). For the GPBoost models, we optimized the parameters learning_rate, min_data_in_leaf, max_depth, and lambda_l2. The grid for model tuning was determined manually by preliminary runs, and the optimization was carried out using the optimization function provided with the *gpboost* R package. The loss function of the hyperparameter optimization for both model types was root-mean-square error.

Assisting models were fitted using NFI plot data alone (NFI), FMI plot data alone (FMI), and both datasets together. We refer to global models when the training data comprised all FMI plots of the study area in model fitting. The local models referred to models that were trained using FMI plots located in the municipality of interest. Mixed-effects models and GPBoost models were considered as global models that are localized to the municipality of interest using a random effect. The NFI plots were used to construct models that only used field plots located in the 20 km buffer zone that surrounded the municipality of interest. The assisting models are described in Table 3.

For the local XGBoost models, the feature importance rankings were determined using the Gain metric. The Gain metric depicts the improvement in accuracy to the branches that the feature is located on. The Gain metric shows the relative contribution of each feature to the reduction of the loss function. We studied the feature importance rankings to investigate whether the most important predictor variables are dissimilar in terms of XGBoost model alternatives or municipalities timber volume estimates.

Volume estimation

Simple expansion estimator

A simple expansion estimator was used to estimate timber volume using only the NFI field data. The expansion estimates for the mean timber volume ($\widehat{\mu}_{\mathrm{EXP}}$, m^3/ha) in a municipality were computed as follows:

$$\widehat{\mu}_{\mathrm{EXP}}(y) = \frac{\sum_{i \in S} y_i}{\sum_{i \in S} n_i} \tag{3}$$

where y_i is the sum of timber volumes (m^3/ha) in the forest plots of cluster i in the NFI sample S for some municipality, and n_i is the number of forest plots in cluster i.

The estimation of variance for $\widehat{\mu}_{\mathrm{EXP}}$ relies on a variant of the Grafström–Schelin estimator (Grafström et al. 2012) computed at the level of the NFI clusters. A Voronoi tessellation was used to tesselate NFI clusters for the determination of local neighborhoods for each NFI cluster, as described in Korhonen et al. (2024). The Grafström–Schelin variance estimator is a local difference estimator that accounts for the spatial autocorrelation by neighborhood. In the Finnish NFI, the variance estimation relies on the cluster-level residuals. The neighborhood was constructed by selecting the center cluster of the neighborhood and the clusters within adjacent Voronoi cells. We omitted neighbor clusters whose Voronoi cells had a touching surface length < 5% in terms of the perimeter of the Voronoi cell of the center cluster. The Grafström–Schelin variance estimator for the volume estimate in a municipality is as follows (see Korhonen et al.

2024):

$$\widehat{\text{var}}\left(\widehat{\mu}_{\text{EXP}}\right) = \frac{1}{\left(\sum_{i\in S} n_i\right)^2} \sum_{i\in S} \frac{m_i}{m_i - 1}\left(z_i - \frac{1}{m_i}\sum_{j\in S_i} z_j\right)^2 \quad (4)$$

where $z_i = y_i - \widehat{\mu}_{\text{EXP}} n_i$, n_i is the number of forest plots in cluster i, and m_i is the number of neighbor clusters in neighborhood S_i for cluster i of NFI sample in municipality S.

The standard error of an estimate in a municipality is

$$\text{SE}\left(\widehat{\mu}_{\text{EXP}}\right) = \sqrt{\widehat{\text{var}}\left(\widehat{\mu}_{\text{EXP}}\right)} \quad (5)$$

Model-assisted estimation

A model-assisted estimator was used with the probability sample of NFI plots and the assisting model to estimate mean volume by municipality. Since the model was always fitted with a different dataset than used for estimation, the model-assisted estimator was known as a difference estimator (Särndal et al. 1992, p. 222, p. 31). The model-assisted estimator combined the model-based mean estimator $\widehat{\mu}_{\text{MB}}(y)$, which is simply the mean of the predicted timber volume in the N grid cells of population U:

$$\widehat{\mu}_{\text{MB}}(y) = \frac{\sum_{l\in U} \widehat{y}_l}{N} \quad (6)$$

with the expansion estimator residual mean ($\widehat{\mu}_{\text{EXP}}$ (e)), to provide a design-unbiased population mean estimator:

$$\widehat{\mu}_{\text{MA}}(y) = \widehat{\mu}_{\text{MB}}(\widehat{y}) + \widehat{\mu}_{\text{EXP}}(\text{e}) = \frac{\sum_{l\in U} \widehat{y}_l}{N} + \frac{\sum_{k\in S} e_k}{\sum_{i\in S} n_i} \quad (7)$$

in which the first component of the estimator is a model-based mean estimate ($\widehat{\mu}_{\text{MB}}$) collected from wall-to-wall volume predictions $\widehat{y}_l$ for N grid cells of municipality U labeled as forest in the forest mask (cell size: 16 m × 16 m), and the second component is a design-based adjustment term that is estimated from the model residuals associated with the NFI field plots of municipality S with $e_k = (y_k - \widehat{y}_k)\, I_k$ for NFI field plot k. I_k is a forest/nonforest indicator variable, i.e., forest mask. The estimated adjustment term corrected the systematic error associated with the predictions produced by the assisting model.

The Grafström–Schelin variance estimator described in eq. 4 were adapted for the model-assisted estimator by replacing the local differences of plot-level volumes with corresponding local differences in residuals as follows:

$$\widehat{\text{var}}\left(\widehat{\mu}_{\text{MA}}\right) = \frac{1}{\left(\sum_{i\in S} n_i\right)^2} \sum_{i\in S} \frac{m_i}{m_i - 1}\left(z_i - \frac{1}{m_i}\sum_{j\in S_i} z_j\right)^2 \quad (8)$$

where $z_i = e_i - \bar{e}\, n_i$ and $z_j = e_j - \bar{e}\, n_j$ refer to residuals of model residuals computed at the level of the NFI clusters in the municipality S or in the local neighborhood S_i.

Performance assessment

For the performance assessment, we filtered out municipalities that comprised <20 NFI clusters. We also minimized the possible effect of municipality area on the precision of the estimates by restricting municipality area to the range 760–1265 km^2 (mean municipality area: 983 km^2). Selected area range was determined by the range of real municipalities in Finland, which had a 760 km^2 median value and a 1265 km^2 mean municipality size. After filtering, 619 synthetic municipalities were included for performance evaluation. The selected set of municipalities comprised, on average, 180 FMI plots and 26 NFI clusters. The 20 km buffer zones of the municipalities comprised, on average, 458 NFI plots.

We assessed the precision of the municipal-level volume estimates by their variance estimates and 95% CIs. The 95% CIs (computed as 1.96 × standard error) were used to evaluate the uncertainty associated with the volume estimate. The CIs were also used to assess how well the model-based volume estimates (i.e., model-assisted estimate without an adjustment term) agreed with the CIs of the model-assisted estimates. Here, we assumed that the model-based estimate was a pixel-counting estimate aggregated from a forest attribute map, i.e., model-based variance estimates were not available. The estimated variances were used to compute ratios, i.e., relative efficiencies (REs). The REs showed a comparison between two estimator efficiencies. First, we computed REs for the ratio of $\widehat{\text{var}}(\widehat{\mu}_{\text{EXP}})$ and $\widehat{\text{var}}(\widehat{\mu}_{\text{MA}})$. Second, we computed REs to compare the performance of linear regression and the tree-boosting approaches presented in Table 3. The REs were computed as a mean (RE_{mean}) and quantiles (RE_{Q25}, RE_{Q50}, RE_{Q75}) over the municipalities. The REs were interpreted as follows: a value of 1 indicated equal efficiency (i.e., the estimated variances are equal), while a value > 1 suggested an efficiency gain. The REs can also be understood as the number of field plots, given the simple random sampling. For example, an RE value of 2 indicated that variance estimates equal to $\widehat{\text{var}}(\widehat{\mu}_{\text{MA}})$ can be achieved by doubling the number of field plots associated with $\widehat{\text{var}}(\widehat{\mu}_{\text{EXP}})$.

Results

Efficiency gains of multiple regression models

The findings indicated that the use of assisting models resulted in considerable efficiency gains in the estimation of mean timber volume compared to the use of the EXP estimator (Table 4). The mean value of the municipal-level variance estimates associated with $\widehat{\mu}_{\text{EXP}}$ was 110.82 (m^3/ha)^2, whereas the smallest mean value of the variance estimates associated with $\widehat{\mu}_{\text{MA}}$ was reported for $\text{LM}_{\text{NFI,loc}}$ (41.34 (m^3/ha)^2), while $\text{LM}_{\text{NFI,loc}}$ outperformed the other models in terms of the mean RE value that showed the relationship of $\widehat{\text{var}}(\widehat{\mu}_{\text{EXP}})$ and $\widehat{\text{var}}(\widehat{\mu}_{\text{MA}})$.

Efficiency gains of tree-boosting models

A comparison of LMs with corresponding tree-boosting models as RE values is shown in Fig. 3. The assisting model that used tree-boosting instead of the LM improved the precision of volume estimates in some municipalities (Fig. 3).

Table 4. Mean of variance estimates and mean and quartiles of relative efficiencies (REs) for model-assisted estimators that used LMs in the synthetic municipalities ($n = 619$).

Assisting model	Mean $\widehat{\text{var}}(\hat{\mu})$ (m^3/ha)^2	RE_{mean}	RE_{Q25}	RE_{Q50}	RE_{Q75}
–	110.82	–	–	–	–
$LM_{NFI,FMI,loc}$	41.34	3.21	2.06	2.74	3.61
$LM_{NFI,loc}$	41.59	3.18	2.05	2.72	3.60
$LM_{FMI,glo}$	42.75	3.06	2.02	2.59	3.57
$LM_{FMI,loc}$	43.41	3.02	1.99	2.59	3.46
$LME_{FMI,me}$	43.58	3.01	1.96	2.55	3.51

Note: The mean variance of the simple expansion estimator is shown in the first row. The RE values were computed as the simple expansion estimator (numerator) relative to model-assisted estimator (denominator). LM—linear regression model, Q—quartile. NFI, national forest inventory; FMI, forest management inventory; LME, linear mixed effect.

Fig. 3. Violin-box plot comparing the relative efficiencies (REs) of linear regression models to those of the corresponding tree-boosting models in the model-assisted framework. The RE values were computed as the simple expansion estimator (numerator) relative to the model-assisted estimator (denominator). The gray dots show mean values. For model abbreviations, please refer to Table 3.

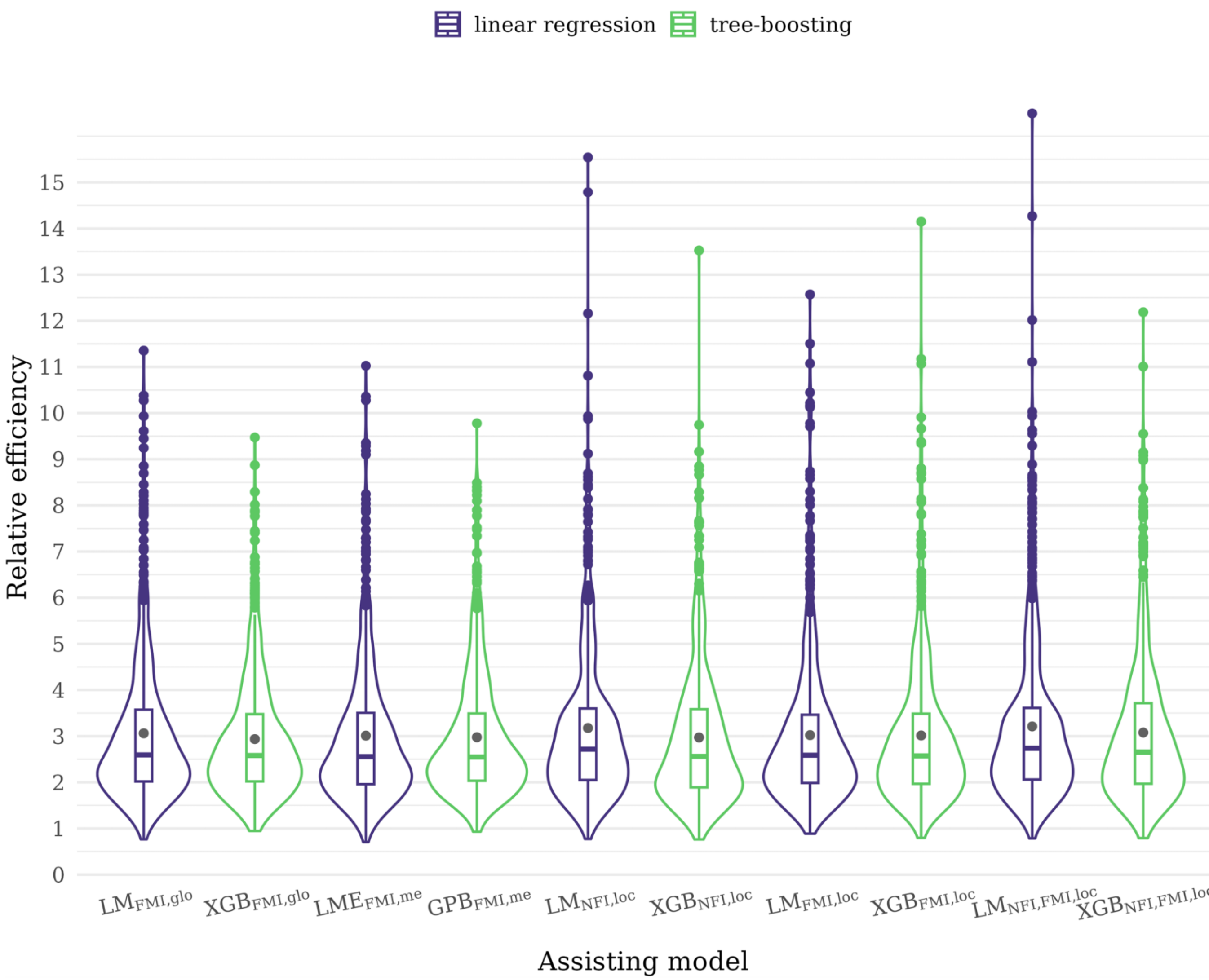

The largest average efficiency gain associated with the use of tree-boosting (instead of LM) was achieved when mixed-effect models were used, namely, $LME_{FMI,me}$ and $GPB_{FMI,me}$. When the efficiency of the model-assisted estimator that used tree-boosting models was compared with the simple expansion estimator (Table 5), we found that the variance estimates were greater than those of the best performing LMs shown in Table 4.

Table 5. Mean of variance estimates and mean and quartiles of relative efficiencies (REs) for model-assisted (MA) estimators that used tree-boosting models in the synthetic municipalities ($n = 619$).

Assisting model	Mean $\widehat{\text{var}}\,(\hat{\mu}_{\text{MA}})$ (m^3/ha)^2	RE_{mean}	RE_{Q25}	RE_{Q50}	RE_{Q75}
–	110.82	–	–	–	–
$\text{GPB}_{\text{FMI,me}}$	42.03	2.98	2.03	2.55	3.49
$\text{XGB}_{\text{NFI,FMI,loc}}$	42.49	3.08	1.97	2.65	3.71
$\text{XGB}_{\text{FMI,loc}}$	43.61	3.01	1.97	2.57	3.49
$\text{XGB}_{\text{FMI,glo}}$	42.8	2.94	2.02	2.58	3.48
$\text{XGB}_{\text{NFI,loc}}$	43.9	2.97	1.89	2.56	3.58

Note: The mean variance of the simple expansion estimator is shown in the first row. The RE values were computed as the simple expansion estimator (numerator) relative to the model-assisted estimator (denominator). LM—linear regression model, Q—quartile. NFI – national forest inventory; FMI – forest management inventory. XGBoost – Extreme Gradient Boosting.

Table 6. Feature importance rankings by timber volume class for the Extreme Gradient Boosting (XGBoost) models.

Municipality volume class (m^3/ha)	Model	Feature importance ranking				
		1	2	3	4	5
96–125	$\text{XGB}_{\text{NFI,loc}}$	z95 (84%)	p15 (83%)	p5 (61%)	s2b8 (39%)	sdz (28%)
	$\text{XGB}_{\text{FMI,loc}}$	z95 (75%)	p15 (66%)	s2b2 (32%)	s2b8 (30%)	sdz (31%)
	$\text{XGB}_{\text{NFI,FMI,loc}}$	z95 (87%)	p15 (86%)	p5 (47%)	s2b8 (31%)	sdz (33%)
125–154	$\text{XGB}_{\text{NFI,loc}}$	z95 (68%)	p15 (62%)	p5 (82%)	sdz (32%)	s2b8 (31%)
	$\text{XGB}_{\text{FMI,loc}}$	z95 (74%)	p15 (55%)	p5 (39%)	s2b10 (21%)	s2b10 (27%)
	$\text{XGB}_{\text{NFI,FMI,loc}}$	z95 (69%)	p15 (65%)	p5 (87%)	s2b8 (34%)	sdz (29%)
154–183	$\text{XGB}_{\text{NFI,loc}}$	z95 (62%)	p15 (50%)	p5 (82%)	s2b2 (41%)	sdz (30%)
	$\text{XGB}_{\text{FMI,loc}}$	z95 (59%)	p15 (46%)	p5 (52%)	s2b10 (24%)	s2b8 (31%)
	$\text{XGB}_{\text{NFI,FMI,loc}}$	z95 (55%)	p15 (49%)	p5 (87%)	s2b2 (39%)	s2b2 (34%)

Note: Volume classification of municipalities is based on simple expansion estimates. Values in parentheses represent the proportion of synthetic municipalities where a feature attained the specified rank. For predictor variable abbreviations, see the "Remotely-sensed data" section. NFI – national forest inventory; FMI – forest management inventory.

Feature importance

Feature importance rankings categorized by equal-width timber volume classes (derived by the simple expansion estimator) for the XGBoost model variants are presented in Table 6. The results indicated that the z95 and p15 features consistently occupied the first and second ranks, respectively, regardless of the model variant or volume class of the municipality. For the 96–125 m^3/ha volume class, these features occupied the same top rankings in over 80% of municipalities. However, this frequency decreased to 49%–50% for the 154–183 m^3/ha volume class. While the top two ranking features remained stable, the third to fifth ranks showed significantly greater variation.

Agreement between model-based estimates and design-based confidence intervals

The assisting models that used the FMI field plots produced adjustment terms that deviated from zero more than the assisting models that used the NFI data (Table 7). The mean adjustment terms were generally moderate, but the standard deviation of adjustment terms revealed fluctuations among municipalities. The greatest mean adjustment term, i.e., greatest level of underprediction, was reported for $\text{XGB}_{\text{FMI,glo}}$ (4.80 m^3/ha), whereas the closest-to-zero adjustment terms were reported for models that used a combination of FMI and NFI data as training data ($\text{LM}_{\text{NFI,FMI,loc}}$, $\text{XGB}_{\text{NFI,FMI,loc}}$). The proportion of model-based volume estimates, i.e., pixel-counting estimates, that fell within the CIs of the model-assisted estimates ranged from 77% to 87%. The strongest agreement (>86%) was observed with the assisting models that used either the global set of FMI plots or the combination of FMI and NFI data in the training phase, whereas the weakest agreement was reported for linear mixed effect (LME) model.

Discussion

Our findings indicated that the model-assisted estimator increased efficiency by 66%–69% relative to the simple expansion estimator. The use of the FMI field plots to fit assisting models enabled model localization in the subdomain of interest, which can be combined with independent residuals from NFI plot measurements for model-assisted estimation (a survey sample-based adjustment of the model predictions). Model-assisted inference is also feasible using only NFI data. In this study, we excluded NFI plots from the region of interest when we fitted the assisting model; only using the NFI model residuals from the area of interest for estimation. Despite not using observations in the region of interest for model fitting, the NFI model model-assisted

Table 7. Mean and standard deviation (SD) of adjustment terms associated with the municipal-level volume estimator.

Assisting model	Mean adjustment term (m^3/ha)	SD of adjustment terms (m^3/ha)	Proportion of model-based estimates in agreement with 95% MA_{CI} (%)
$XGB_{FMI,glo}$	4.80	8.74	81.58
$XGB_{FMI,loc}$	4.15	9.40	77.22
$LM_{FMI,glo}$	3.27	8.13	86.11
$LM_{FMI,loc}$	2.61	8.99	82.88
$GPB_{FMI,me}$	2.30	8.79	83.36
$LME_{FMI,me}$	0.82	10.17	76.58
$LM_{NFI,FMI,loc}$	− 0.18	8.32	85.78
$XGB_{NFI,FMI,loc}$	− 0.43	8.44	86.59
$LM_{NFI,loc}$	− 1.45	8.85	82.23
$XGB_{NFI,loc}$	− 1.92	8.92	79.48

Note: The rightmost column shows the agreement of model-based estimates with the confidence intervals (CIs) of the model-assisted (MA) estimates. For model abbreviations, please refer to Table 3. NFI – national forest inventory; FMI – forest management inventory. XGBoost – Extreme Gradient Boosting; LM – linear regression model.

estimator $LM_{NFI,loc}$ still outperformed the localized FMI model ($LM_{FMI,loc}$), which was fitted with plots inside the region of interest.

The localization of global models to small subdomains can also be carried out using the estimated best unbiased linear predictor approach from the context of model-based inference (Kangas et al. 2025). This approach is often applied in cases where the subdomain is comprised of a small number of field plots, and estimation increases the contribution of the model predictions. The random effect allows for contiguous spatial regions (e.g., a municipality) to have higher or lower average predictions. In our case, localization of a global assisting model with random effects in a mixed model ($LM_{FMI,me}$ and $GPB_{FMI,me}$) did not improve the estimator efficiency compared to estimation with a global assisting model and no random effects. This suggests a homogeneity across the study region with respect to modeled relationships, possibly due to the high level of variability explained by remote sensing. It is also worth noting that the municipalities were synthetically generated, and municipalities of the pooled set (619 municipalities) geographically overlapped due to the somewhat limited study region (1.56 million ha) used for the simulation of synthetic municipalities. This means that aspects of administrative decisions, such as forest management regimes, could not be accounted for in this analysis. The limited study region also means that the estimated range of conditions reflected in the RE values (RE_{75}–RE_{25}) and deviations of the adjustment terms are likely smaller compared to actual municipality data over large areas.

Our findings suggest that NFI plots in the 20 km buffer zone around the municipality of interest can be used for efficient municipal-level model-assisted estimations. This is an important implication for small regions that may have an insufficient number of internal plots for robust model fitting. For example, Cochran (1977) recommended that a minimum of 20 observations (relevant to the idea of 20 plot clusters in the Finnish NFI) are needed for design-based inference and associated variance estimation per stratum. In the smallest municipalities with few or no plots, model-based small-area estimators that leverage models trained over a larger region are needed for municipal-level remote sensing augmented estimates. Kangas et al. (2025) indicated that identification of optimal localization strategies for model-based estimation is a challenge due to potential tradeoffs in bias and precision: an unbiased estimator may be imprecise while a precise estimator may be biased. We encountered exactly this phenomenon in this study; while precision gains were considerable, bias was evident from the fact that 95% CI coverage probabilities for model-based volume estimates were only 77%–87%.

Our study found that models fitted to the FMI plots had, on average, a larger magnitude of adjustment terms, associated with the difference estimator, than models fitted to the NFI plots. This is consistent with the different objectives for FMI and NFI sample plots. The former are a nonprobability (purposive) sample targeted toward regions of active timber production, while the latter represent a systematic grid sample of all forest types. It is also worth noting that each FMI field plot is always located completely within a forest stand, whereas NFI plots may be split between different forest development stages or between forest and nonforest areas. It is not surprising then that FMI models may be biased for NFI-plot based estimates, which represent a broader range of forest types. We did not assess the performance of the two model types on timber production lands.

Although ALS point clouds are generally perceived to perform better than imagery-based point clouds for forest inventory modeling, cost and logistical considerations motivated us to use imagery-based point clouds for this study. While ALS data are also available for large areas in Finland, they are collected less frequently than imagery due to the high cost of the ALS data. This means that there is generally better temporal agreement between field plots and imagery-based point clouds. Unfortunately, given the periodicity of remote sensing programs and the annualized nature of NFI and FMI forest measurements, even imagery-based point clouds suffer some temporal mismatches with the field measurements. We mitigated the growth-related temporal discrepancies by projecting the NFI data to the mid-year of our 3-year aerial imaging period. Forest treatments, such as clear cuts and thinnings, were not considered in this investigation because they are not catalogued as a census, and remote sensing tools struggle to identify them. However, this could be an opportunity for future improvements.

Photogrammetric point clouds appear similar to ALS point clouds, but they are inherently different in how they are collected and in how they interact with the forest structure. Many studies have demonstrated that a key limitation of photogrammetric point clouds is that they predominantly describe the canopy surface, while ALS can penetrate the canopy and provide subcanopy structure information (White et al. 2013; Rahlf et al. 2017). A consequence of this limitation in photogrammetric point clouds is that an ALS-derive terrain model is generally needed to compute forest height. There are also computational differences with photogrammetric point clouds, such as the standard height thresholds used with ALS data, e.g., the ratio of returns above 2 m to all return ("2 m cover ratio"); there frequently may not be any points below 2 m.

In our findings, the performances of linear regression and tree-boosting approaches were practically equivalent, although it is possible that additional explanatory power is feasible with tree-boosting. To ensure a fair comparison, we used a fixed set of predictor variables for both linear regression and tree-boosting to eliminate variable selection as a source of confounding. In practice, however, tree-boosting may be improved through the use of all available predictors. Tree-boosting models tend to be robust to overfitting (Cosenza et al. 2021). However, there is still cause for concern with overfitting as some of the municipalities had as few as 41 observations. The performance of tree-boosting could be potentially improved by carrying out hyperparameter tuning for each municipality. However, this may further increase the risk of overfitting in the absence of an independent tuning dataset. In this study, the hyperparameters were optimized once using cross-validation and the global set of FMI plots. For local XGBoost models, we analyzed the rankings of the top five important predictor variables that remained stable regardless of the mean volume of municipality and the tree-boosting model variant. The findings highlighted the role of the height-related features derived from the photogrammetric points clouds over the Sentinel-2 features in the assisting models.

While our findings demonstrate efficiency gains from employing FMI field plots in addition to NFI plots, the slight improvements did not appear to warrant the added complexity required to incorporate this additional dataset. Fitting models with only NFI data leads to nearly identical efficiency gains when compared to a combined NFI and FMI estimation strategy. In future research, we will investigate how the width of the buffer zone used to collect the NFI plots for the training of an assisting model affects the precision of municipal-level estimates. Finally, the proposed model-assisted estimation framework that used photogrammetric point clouds will also be comprehensively tested in real municipalities with dissimilar forest characteristics and for other forest attributes.

Conclusions

We estimated municipal-level timber volume using a model-assisted framework that employed either linear regression or tree-boosting assisting models. The assisting models were fitted using NFI plots collected from surrounding areas of the municipalities and/or FMI plots coupled with aerial image-based point clouds and Sentinel-2 images. From this investigation we can draw the following conclusions:

1. The model-assisted estimator with photogrammetric point clouds produced mean relative efficiencies that ranged from 2.9 to 3.2 in the estimation of municipal-level mean volume compared to estimation without remote sensing.
2. The localization of the assisting models that used FMI field plots and random effects for municipalities did not appreciably improve estimator efficiency, likely due to the homogeneity of the forests and the nature of the synthetic municipalities.
3. Performances of linear regression and tree-boosting models were equivalent.
4. The greatest efficiency gains were achieved with an assisting model that used a combination of NFI and FMI data, although improvements relative to using NFI alone were slight. This suggests that the effort needed to process and integrate the two disparate FMI and NFI datasets is not worth the considerable additional effort.

Acknowledgements

We acknowledge Timo Pitkänen for his technical expertise regarding the processing of the satellite data. The work was financed by the Ministry of Agriculture and Forestry through *Catch the carbon* research and innovation programme (KUNTANIELU project). The work was also supported by the Research Council of Finland through the Finnish Flagship Programme for *the Forest-Human-Machine Interplay—Building Resilience, Redefining Value Networks and Enabling Meaningful Experiences* (UNITE) [359174], and the project *Asynchronous datasets in large-area forest inventories by remote sensing* (ASYNC) [355267].

Article information

History dates

Received: 7 November 2025
Accepted: 9 March 2026
Version of record online: 27 April 2026

Copyright

Data availability

The data that support the findings of this study are available from the corresponding author upon a reasonable request.

Author information

Author ORCIDs

Janne Räty https://orcid.org/0000-0002-6578-8965
Mikko Kukkonen https://orcid.org/0000-0003-4206-1680
Annika Kangas https://orcid.org/0000-0002-8637-5668
Raisa Mäkipää https://orcid.org/0000-0003-3146-4425

Author contributions

Conceptualization: JR, MK, AK, JS, RM, PP
Data curation: JR, MK
Formal analysis: JR
Methodology: JR, MK
Project administration: RM, PP
Resources: RM, PP
Supervision: RM, PP
Writing – original draft: JR, MK
Writing – review & editing: MK, AK, JS, RM, PP

Competing interests

The authors declare there are no competing interests.

References

Agisoft. 2024. AgiSoft Metashape Professional (Version 2.0.3 build 16960) (Software).

Bohlin, J., Wallerman, J., and Fransson, J.E.S. 2012. Forest variable estimation using photogrammetric matching of digital aerial images in combination with a high-resolution DEM. Scand. J. For. Res. **27**: 692–699. doi:10.1080/02827581.2012.686625.

Breidenbach, J., and Astrup, R. 2012. Small area estimation of forest attributes in the Norwegian National Forest Inventory. Eur. J. For. Res. **131**: 1255–1267. doi:10.1007/s10342-012-0596-7.

Chen, T., He, T., Benesty, M., Khotilovich, V., Tang, Y., Cho, H., et al. 2025. XGBoost: Extreme Gradient Boosting. doi:10.32614/CRAN.package.xgboost.

Cochran, W. 1977. Sampling techniques. 3rd ed. Wiley, New York.

Copernicus Data. 2023. Copernicus data space ecosystem.

Cosenza, D.N., Korhonen, L., Maltamo, M., Packalen, P., Strunk, J.L., Næsset, E., et al. 2021. Comparison of linear regression, *k*-nearest neighbour and random forest methods in airborne laser-scanning-based prediction of growing stock. Forestry, **94**: 311–323. doi:10.1093/forestry/cpaa034.

Erenoglu, R.C. 2017. Reliability of GPS/GNSS-based positioning in a forestry environment. J. For. Res. **28**: 605–614. doi:10.1007/s11676-016-0332-0.

Fabio, S., Tim, G., and Pascal, K. 2021. GPboost: combining tree-boosting with gaussian process and mixed effects models.

Grafström, A., Lundström, N.L.P., and Schelin, L. 2012. Spatially balanced sampling through the pivotal method. Biometrics, **68**: 514–520. doi:10.1111/j.1541-0420.2011.01699.x.

Haakana, H., Heikkinen, J., Katila, M., and Kangas, A. 2020. Precision of exogenous post-stratification in small-area estimation based on a continuous national forest inventory. Can. J. For. Res. **50**: 359–370. doi:10.1139/cjfr-2019-0139.

Hawryło, P., and Wężyk, P. 2018. Predicting growing stock volume of Scots Pine stands using Sentinel-2 satellite imagery and airborne image-derived point clouds. Forests, **9**. doi:10.3390/f9050274.

Irulappa-Pillai-Vijayakumar, D.B., Renaud, J.-P., Morneau, F., McRoberts, R.E., and Vega, C. 2019. Increasing precision for French forest inventory estimates using the k-NN technique with optical and photogrammetric data and model-assisted estimators. Remote Sens. **11**: 991. doi:10.3390/rs11080991.

Kangas, A., Myllymäki, M., Gobakken, T., and Næsset, E. 2016. Model-assisted forest inventory with parametric, semiparametric, and nonparametric models. Can. J. For. Res. **46**: 855–868. doi:10.1139/cjfr-2015-0504.

Kangas, A., Pitkänen, T.P., Mehtätalo, L., and Heikkinen, J. 2022. Mixed linear and non-linear tree volume models with regional parameters to main tree species in Finland. Forestry, **96**: 188–206. doi:10.1093/forestry/cpac038.

Kangas, A., Myllymäki, M., and Packalen, P. 2025. Small area estimators in a simulation test. Can. J. For. Res. **55**: 1–17. doi:10.1139/cjfr-2024-0070.

Karhinen, S., Peltomaa, J., Riekkinen, V., and Saikku, L. 2021. Impact of a climate network: the role of intermediaries in local level climate action. Global Environ. Change, **67**: 102225. doi:10.1016/j.gloenvcha.2021.102225.

Korhonen, K.T., Räty, M., Haakana, H., Heikkinen, J., Hotanen, J.-P., Kuronen, M., and Pitkänen, J. 2024. Forests of Finland 2019–2023 and their development 1921–2023. Silva Fenn.

Kuhn, M. 2025. tune: tidy tuning tools. doi:10.32614/CRAN.package.tune.

Mäkisara, K., Katila, M., and Peräsaari, J. 2022. The multi-source National Forest Inventory of Finland—methods and results 2017 and 2019. *In* Natural resources and bioeconomy studies. Vol. 73.

Maltamo, M., and Packalen, P. 2014. Species-specific management inventory in Finland. *In* Forestry Applications of Airborne Laser Scanning. Managing Forest Ecosystems. **vol 27**. *Edited by* M. Maltamo, E. Næsset and J. Vauhkonen. Springer, the Netherlands, Dordrecht. doi:10.1007/978-94-017-8663-8_12.

Massey, A., Mandallaz, D., and Lanz, A. 2014. Integrating remote sensing and past inventory data under the new annual design of the Swiss National Forest Inventory using three-phase design-based regression estimation. Can. J. For. Res. **44**: 1177–1186. doi:10.1139/cjfr-2014-0152.

McRoberts, R.E., Næsset, E., Heikkinen, J., Chen, Q., Strimbu, V., Esteban, J., et al. 2022. On the model-assisted regression estimators using remotely sensed auxiliary data. Remote Sens. Environ. **281**: 113168. doi:10.1016/j.rse.2022.113168.

Mehtätalo, L., and Lappi, J. 2020. Biometry for forestry and environmental data with examples in R. CRC Press. doi:10.1201/9780429173462.

Metsäkeskus, S. 2024. Inventointikoealat.

Myllymäki, M., Gobakken, T., Næsset, E., and Kangas, A. 2017. The efficiency of poststratification compared with model-assisted estimation. Can. J. For. Res. **47**: 515–526. doi:10.1139/cjfr-2016-0383.

National Land Survey of Finland. 2025. Laserkeilaus ja ilmakuvaus.

Opsomer, J.D., Breidt, F.J., Moisen, G.G., and Kauermann, G. 2007. Model-assisted estimation of forest resources with generalized additive models. J. Am. Stat. Assoc. **102**: 400–409. doi:10.1198/016214506000001491.

Pinheiro, J., and Bates, D., R Core Team. 2025. nlme: linear and nonlinear mixed effects models. https://doi.org/10.32614/CRAN.package.nlme. R package version 3.1-168

Pitkänen, T.P., Balazs, A., and Tuominen, S. 2024. Automatized Sentinel-2 mosaicking for large area forest mapping. Int. J. Appl. Earth Obs. Geoinformation, **127**: 103659. doi:10.1016/j.jag.2024.103659.

Pitt, D.G., Woods, Murray, and Penner, M. 2014. A comparison of point clouds derived from stereo imagery and airborne laser scanning for the area-based estimation of forest inventory attributes in boreal Ontario. Can. J. Remote Sens. **40**: 214–232. doi:10.1080/07038992.2014.958420.

Puliti, S., Breidenbach, J., and Astrup, R. 2020. Estimation of forest growing stock volume with UAV laser scanning data: can it be done without field data? Remote Sens. **12**: 1245. doi:10.3390/rs12081245.

Puliti, S., Breidenbach, J., Schumacher, J., Hauglin, M., Klingenberg, T.F., and Astrup, R. 2021. Above-ground biomass change estimation using national forest inventory data with Sentinel-2 and Landsat. Remote Sens. Environ. **265**: 112644. doi:10.1016/j.rse.2021.112644.

Pulkkinen, M., Ginzler, C., Traub, B., and Lanz, A. 2018. Stereo-imagery-based post-stratification by regression-tree modelling in Swiss National Forest Inventory. Remote Sens. Environ. **213**: 182–194. doi:10.1016/j.rse.2018.04.052.

R Core Team. 2025. R: a language and environment for statistical computing. R Foundation for Statistical Computing, Vienna, Austria.

Rahlf, J., Breidenbach, J., Solberg, S., Næsset, E., and Astrup, R. 2017. Digital aerial photogrammetry can efficiently support large-area forest inventories in Norway. Forestry, **90**: 710–718. doi:10.1093/forestry/cpx027.

Saarela, S., Grafström, A., Ståhl, G., Kangas, A., Holopainen, M., Tuominen, S., et al. 2015. Model-assisted estimation of growing stock volume using different combinations of LiDAR and Landsat data as auxiliary information. Remote Sens. Environ. **158**: 431–440. doi:10.1016/j.rse.2014.11.020.

Särndal, C.-E., Swensson, B., and Wretman, J. 1992. Model assisted survey sampling. Springer Science & Business Media.

Schroeder, T.A., Obata, S., Papeş, M., and Branoff, B. 2022. Evaluating statewide NAIP photogrammetric point clouds for operational improvement of national forest inventory estimates in mixed hardwood forests of the southeastern U.S. Remote Sens. **14**: 4386. doi:10.3390/rs14174386.

White, J.C., Wulder, M.A., Vastaranta, M., Coops, N.C., Pitt, D., and Woods, M. 2013. The utility of image-based point clouds for forest inventory: a comparison with airborne laser scanning. Forests, **4**: 518–536. doi:10.3390/f4030518.